Semiconductor nanostructures in biological applications

2005 J. Phys.: Condens. Matter 17 R637

(http://iopscience.iop.org/0953-8984/17/26/R01)

INSTITUTE OF PHYSICS PUBLISHING JOURNAL OF PHYSICS: CONDENSED MATTER

J. Phys.: Condens. Matter **17** (2005) R637–R656 doi:10.1088/0953-8984/17/26/R01

TOPICAL REVIEW

Semiconductor nanostructures in biological applications

Dimitri Alexson[1], Hongfeng Chen[2], Michael Cho[2,3], Mitra Dutta[1,3], Yang Li[1], Peng Shi[2], Amit Raichura[1], Dinakar Ramadurai[2], Shaunak Parikh[2], Michael A Stroscio[1,2,3,4] and Milana Vasudev[2]

[1] Department of Electrical and Computer Engineering, University of Illinois at Chicago, Chicago, IL 60607, USA
[2] Department of Bioengineering, University of Illinois at Chicago, Chicago, IL 60607, USA
[3] Department of Physics, University of Illinois at Chicago, Chicago, IL 60607, USA

E-mail: stroscio@uic.edu

Received 4 January 2005, in final form 21 March 2005
Published 17 June 2005
Online at stacks.iop.org/JPhysCM/17/R637

Abstract

Semiconductor nanostructures in biological applications are discussed. Results are presented on the use of colloidal semiconductor quantum dots both as biological tags and as structures that interact with and influence biomolecules. Results are presented on the use of semiconducting carbon nanotubes in biological applications.

(Some figures in this article are in colour only in the electronic version)

Contents

1. Introduction

The applications of semiconductor nanocrystals in biotechnology have been highlighted recently by a broad variety of applications (Stroscio and Dutta 2004, Jovin 2003) in the study of subcellular processes of fundamental importance in biology. These applications include the use quantum dots as a new type of fluorescent probes as well as their use as

[4] Author to whom any correspondence should be addressed.

active electronic and optical components in nanostructure–biomolecule complexes of potential utility in influencing bimolecular processes in cells (Rajh *et al* 2004). Likewise, carbon nanotubes (CNTs) portend many applications in nanobiotechnology as a result of their nanoscale diameters and as a result of the fact that they may be produced as metallic or semiconducting nanostructures. Sethuraman *et al* (2004) have surveyed potential applications of carbon nanotubes in bioengineering and have reviewed the basic structural and electronic properties of carbon nanotubes.

Fluorescence microscopy is a well established, sensitive, high-resolution method for biological research, and has become one of the cornerstones of real-time imaging of living cells and a powerful tool for cell biologists. This status relies greatly on the availability of sensitive and selective fluorescent probes, also called fluorophores or fluorochromes. Among the routinely employed fluorescent probes are chemical fluorophores, such as fluorescein and phycoerythrin. Though they have been used for many years, these fluorophores usually have one or more deficiencies, including sensitivity to environmental pH changes, susceptibility to photobleaching, fixed emission spectra, and limited Stokes shifts—separations between excitation and emission maxima—which interfere with the detection of a fluorochrome (Javois 1999, Kasten 1999). An example of the progress made in the development and use of fluorescent probes is the discovery of green fluorescent protein (GFP) and its variants. Significant advantages of fluorescent protein-based indicators over simple organic dyes are that they may be designed to respond to a much greater variety of biological events and signals, may be targeted to subcellular compartments, may be introduced into a wider variety of tissues and intact organisms, and are very rarely the cause of photodynamic toxicity (Zhang *et al* 2002). Although investigators continue to engineer new GFP mutants yielding brighter more red-shifted spectra, GFP-like probes suffer from the drawback that they have a narrow excitation spectrum and emit light over a relatively wide range (Kasten 1999). These properties render them difficult to use for multiple-labelling applications since they require simultaneous excitation and collection of fluorescent signals.

In recent years, advances in nanomaterials have produced a new class of fluorescent probes by conjugating semiconductor quantum dots (QDs), also known as semiconducting nanocrystals, with biomolecules that have affinities for binding with selected biological structures. These inorganic dyes have great advantages (Alivisatos 1996, Klarreich 2001) over conventional organic dyes; such advantages include the option for continuously and precisely tuning the emission wavelength of quantum dots by changing the size of the nanocrystal; narrow symmetric emission spectra; a single light source can be used for simultaneous excitation of multiple semiconductor quantum dots with different emission spectra of longer wavelengths than the source; ability to function through repeated cycles of excitation and fluorescence for hours; and extreme stability of coated quantum dots against photobleaching as well as changes in the pH of the biological electrolytes that are ubiquitous in biological environments. These novel optical properties render quantum dots ideal fluorophores for ultrasensitive, multicolour, and multiplexing applications in cell and molecular biology as well as in bioengineering.

Similar studies with carbon nanotubes (CNTs) have emphasized the use of chemically functionalized CNTs to achieve specificity in binding to biological structures (Chen *et al* 2001) and how an electrolyte facilitates the control of the electrical properties of a CNT (Kruger *et al* 2001).

2. Semiconductor quantum dots: chemical functionalization for biological applications

The use of quantum dots as fluorescent probes in biological environments poses special challenges; these include designing and fabricating semiconductor quantum dots that remain

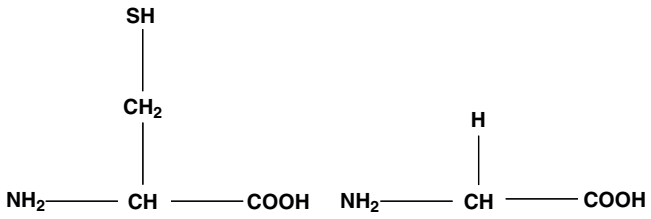

Figure 1. Cysteine is depicted on the left and glycine on the right; the cysteine amino acid has a side group containing a sulfur atom and the glycine amino acid has a relatively simple side group that contains just one hydrogen atom.

fluorescent in aqueous environments and the conjugation of quantum dots with molecules that have an affinities for binding to specific biological structures. To address the first challenge, quantum dots are usually functionalized by certain organic compounds such as mercaptoacetic acid (Chan and Nie 1998) or coated with a hydrophilic layer such as silica (Bruchez *et al* 1998). in order to make them water soluble. Concerning the second problem, many schemes have been successfully realized (Chan *et al* 2002) for conjugating QDs with biomolecules that bind selectively to specific subcellular structures. One specific strategy for functionalizing QDs involves conjugating CdS QDs or ZnS-capped CdSe QDs with peptide sequences with certain motifs. Peptides are short-length proteins that are composed of strings of amino acids. The 20 amino acids are alanine (A), arginine (R), asparagine (N), aspartic acid (D), cysteine (C), glutamine (Q), glutamic acid (E), glycine (G), histidine (H), isoleucine (I), leucine (L), lysine (K), methionine (M), phenylalanine (F), proline (P), serine (S), threonine (T), tryptophan (W), tyrosine (Y), and valine (V). The 20 amino acids all have a basic structure of a molecule with an NH_2 group (amine group), on one end, and with a COOH group (carboxyl group) on the other end; there is a carbon atom between these end groups and bound to the carbon atom are a hydrogen atom and a side group; all amino acids differ only in their side groups. As shown in figure 1, the cysteine amino acid has a side group containing a sulfur atom and the glycine amino acid has a relatively simple side group that contains just one hydrogen atom. The sulfur in the side group of the cysteine molecule plays a special role in protein folding: the side groups of two cysteine amino acids in a protein exhibit the strongest bond associated with protein folding, namely the sulfur–sulfur bond known as a thiol bond. Consequently, folded proteins have strong bonds where the sulfur in the side arm of one cysteine binds to the side arm of another cysteine. Likewise, a peptide such as CGGGRGDS or CGGGGLDV will have a strong affinity for binding to a CdS or ZnS-coated CdSe quantum dot through a thiol bond. For peptides such as GGGGRGDS or GGGGLDV, without a sulfur-containing side group, another widely used method for binding to quantum dots relies on functionalizing the quantum dot with a ligand that binds to the quantum dot and contains a carboxyl group or an amine group. The cross-linking process in this procedure results in the covalent bonding of the carboxyl (or amine) group present in the ligand on the quantum dot to an amine (or carboxyl) group on a biomolecule; since many of the important types of molecules—peptides, proteins, antibodies, and DNA—contain such carboxyl and amine groups, this procedure opens the way to functionalizing quantum dots with a wide variety of biomolecules. Indeed, proteins are found ubiquitously in biological functions and processes; antibodies (a subset of all proteins) bind with high selectivity to specific molecular targets—known as antigens. The cross-linking reagents of use in functionalizing quantum dots in this manner contain reactive ends for specific functional groups (amine and carboxyl groups). Cross-linking reagents used widely in binding biomolecules to quantum dots are EDC (1-ethyl-3-(3-dimethylaminopropyl)

carbodiimide hydrochloride) and sulfo-NHS (N-hydroxysuccinimide). In the case of quantum dots functionalized with carboxyl groups, EDC reacts with the carboxylic acid group and activates the carboxyl group to form an active O-acylisourea intermediate, allowing it to be coupled to the amino group in the reaction mixture. An EDC by-product is released as a soluble urea derivative after displacement by the nucleophile. The O-acylisourea intermediate is unstable in aqueous solutions, making it ineffective in two-step conjugation procedures without increasing the stability of the intermediate using N-hydroxysuccinimide. This intermediate reacts with a primary amine to form an amide derivative (Hermanson 1996). Through this procedure peptides such as GGGGRGDS or GGGGLDV may be bound to carboxyl-functionalized quantum dots (QDs) in the configurations QD-GGGGRGDS and QD-GGGGLDV, since the terminus of the glycine (G) contains an amine group. Likewise, GGGGRGDS or GGGGLDV may be bound to amine-functionalized quantum dots (QDs) in the configurations GGGGRGDS-QD and GGGGLDV-QD, since the terminus of the serine (S) contains a carboxyl group as does valine (V). These QD–peptide conjugates find many uses in binding to a variety of cellular structures because different peptides have binding affinities to selected biomolecules known as integrins, receptors, and ion channels. These integrins, receptors, and ion channels generally span the bilipid layer that forms the several-nanometre-thick cellular membrane and are referred to frequently as transmembrane proteins.

Among the functions of integrins are the binding—or attachment—of cells to extracellular matrices (ECMs) as well as the adhesion of cells to cells. These integrins are heterodimers composed of α-coil and β-sheet protein subunits, which are noncovalently associated with each other. Generally, both of these subunits are transmembrane glycoproteins with relatively large extracellular domains and short tails in the cytoplasmic interior of the cell. Seventeen different α and eight β subunits are known currently, these subunits associate to form at least 23 different integrin heterodimers. They serve as integral cell membrane receptors that form contacts with various ECM-ligands (i.e., the collagens, entactin, fibronectin, fibrinogen, laminin, thrombospondin, virtronectin, and intercellular adhesion molecules) (Alberts *et al* 2002, Mizejewski 1999). Individual ligands are often recognized by several integrins and individual integrins can often bind to more than one ligand. There are some specific sites in the ligands which integrins can recognize. A particularly well known binding site is the Arg–Gly–Asp (RGD) amino acid sequence in fibronectin, vitronectin, and a variety of other proteins; this peptide sequence is recognized by several integrins ($\alpha_5\beta_1$, $\alpha_{\mathrm{II}b}\beta_3$, and most $\alpha_{\mathrm{v}}\beta$ integrins) (Hynes 1992). In addition to RGD (Mizejewski 1999, Hynes 1992, Ruoslahti 1996, Stroscio and Dutta 2004), other sequences are recognized by different integrins: $\alpha_2\beta_1$ binds Asp–Gly–Glu–Ala (DGEA); $\alpha_4\beta_1$ recognizes Leu–Asp–Val (LDV); $\alpha_{\mathrm{II}b}\beta_3$ binds to Lys–Gln–Ala–Gly–Asp–Val (KQAGDV); $\alpha_2\beta_1$ associates with Phe–Tyr–Phe–Asp–Leu–Arg (FYFDLR) and Tyr–Tyr–Gly–Asp–Ala–Leu–Arg (YYGDALR); and $\alpha_4\beta_1$ recognizes Ile–Asp–Ala(Pro–Ser) (IDA(PS)) and Arg–Glu–Asp–Val (REDV). Moreover, the peptides Ile–Lys–Val–Ala–Val (IKVAV) and Ser-Ile–Lys–Val–Ala–Val (SIKVAV) are known to bind to neurons (Powell and Kleinman 1997). The binding of a such a peptide-functionalized quantum dot to a transmembrane intergrin is illustrated in figure 2.

3. Role of semiconductor physics in biological applications of quantum dots

Quantum dots are nanometre-scale semiconductor particles that are neither small molecules nor bulk solids. Their composition and small size (a few hundred to a few thousand atoms, but frequently with radii less than the exciton Bohr radii) cause these dots to have extraordinary electronic, optical, and mechanical properties, which have been investigated by a broad community of scientists and engineers for over a decade (Stroscio and Dutta 2001, Chen

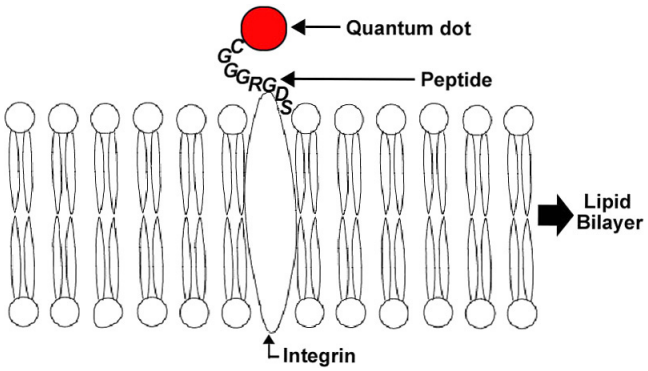

Figure 2. Schematic diagram of peptide-directed QDs binding to an integrin spanning the bilipid cellular membrane.

et al 2000, Empedocles *et al* 1996, Hines and Guyot-Sionnest 1996, Kuno *et al* 2000, Schmidt *et al* 1997, Zhang *et al* 1998, Micic *et al* 1999, Nenadovic *et al* 1990, Machol *et al* 1993, Wehrenberg *et al* 2002). Semiconductor quantum dots have received considerable attention in connection with their uses as nanoscale fluorescent markers. Of course, one of the dominant physical characteristics of a pure, defect-free semiconductor is that it exhibits a gap in energy, E_{gap}, where no states exist. Above this energy gap is a band of energy states known as the conduction band, and below the energy gap is a band of energy states known as the valence band. Traditionally, the lowest energy in the conduction band of an idealized one-dimensional semiconductor is denoted by E_{c} and the highest energy in the valence band by E_{v}.

A simple but useful model of the energy states in such a nanocrystal is based on treating the electrons and holes as being trapped within the diameter of the nanocrystal in an infinitely deep one-dimensional quantum well; that is, E_{c} is taken to have an infinite value outside the region $0 < x < d$ (d is the diameter of the well) and a zero value inside the well. The stationary states, E_n, of a particle of mass m in such a well are given by

$$E_n = \frac{n^2\pi^2\hbar^2}{2md^2}, \qquad n = 1, 2, 3 \ldots \tag{1}$$

where n is known as the quantum number and $\hbar$ is the Planck constant divided by 2π. For a macroscopic semiconductor, the energy states just above the conduction band edge are treated as continuous since the number of atoms—and therefore states—is very large and since confinement effects are small. However, for a quantum dots, the number of atoms—and therefore states—is limited, and confinement effects yield the discrete spectrum of equation (1).

For a spherical quantum dot, the confinement occurs in three dimensions. It turns out that the ground state energy, E_1, of a particle of mass m in an infinitely deep spherical well is given by simply replacing the width of the one-dimensional well, d, with the radius of the quantum dot. When the quantum dots of interest function as luminescent biotags, an electron in a full valence band is 'excited' or elevated from the valence band to the conduction band by a photon of energy $h\nu$, where h is Planck's constant and ν is the frequency of the photon, or equivalently, the frequency of the light, and a hole is left in the valence band. The lowest energy possible for this photon is

$$h\nu = \frac{h^2}{2m_{\text{e}}a^2} + \frac{h^2}{2m_{\text{h}}a^2} + E_{\text{gap}} \tag{2}$$

where the first two terms on the right side of this equation represent the ground state energies of an electron of mass m_{e} and the hole of mass m_{h} in the quantum dot of radius, a, and

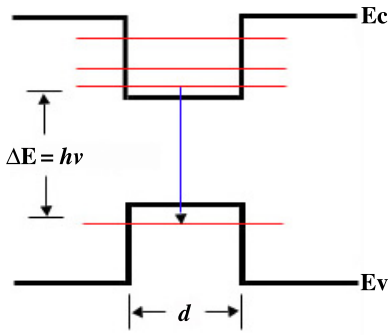

Figure 3. Diagram of bandgap theory and photoluminescence.

E_{gap} is the energy difference between the conduction and valence band edges. In practice, the energy of the lowest possible transition is altered by several additional factors (Stroscio and Dutta 2004): the electron and hole produced by the radiation are attracted to each other through a Coulomb attraction that lowers their energy by an amount that is generally tens of millielectronvolts depending on the material; the potential wells are not infinitely deep and the infinitely-deep-well approximation is not strictly valid, leading to the need for a numerical solution of a transcendental equation for the energy eigenvalues (Liboff 1980, Banyai and Koch 1993); relative effects of both excitonic confinement and dimensional confinement must be considered; dielectric screening must be taken into account when the quantum dot is layered with materials of different dielectric constants and immersed in a liquid of a specific dielectric constant ($\varepsilon = 80$ for water); for materials with spontaneous polarizations, internal electric fields lead to bandbending and consequent shifts in the quantum dot energy levels; colloidal quantum dots in electrolytic suspensions—generally the most useful quantum dots in biological applications—have surface charges that depend on the pH of the electrolyte and potential-contributing double layers of opposite charge form in the vicinity of the surface of the quantum dot; deviations from perfect spherical geometry—a pronounced effect for so-called self-assembled quantum dots of approximately pyramidal shape—lead to shifts in the energy states; and the binding of a ligand to the surface of a quantum dot produces a potential-contributing dipole moment that may be tens of Debyes (Rajh *et al* 2002). Nevertheless, the simple approximations leading to equation (2) provide a useful result in understanding the dominant emission line of a semiconductor quantum dot. Figure 3 depicts energy eigenstates for the case of a quantum dot with finite conduction band and valence band well depths.

Excited electrons lose energy through available scattering channels. Figure 3 depicts the frequently dominant energy loss mechanism whereby the excited electron emits a photon and refills an empty valence state known as a hole. As a result of energy loss caused by many factors such as lattice vibrations (Stroscio and Dutta 2001, Chen *et al* 2004) and transitions between energy states in the conduction band, the wavelength of the re-emitted light may be longer than that of the light used to excite the electron from a valence band state to a conduction band state. From equation (2), it is clear that the fluorescent spectrum depends on the energy gap of the semiconductor and the radius of the quantum dot. By selecting different quantum dot materials, it is possible to design quantum dots so that they fluoresce in a particular region of the spectrum. Moreover, by changing the radius of such a quantum dot, additional tuning of the emission spectrum results from dimensional confinement as indicated by equation (1). This leads to the extremely useful result that it is possible to tune the emission of a quantum dot—say CdSe—over the visible region by changing the dot radius. With several CdSe quantum-dot

Table 1. Energy bandgaps and spontaneous polarizations of selected compound semiconductors.

Compound semiconductor	Bandgap (eV)	Spontaneous polarization, (C m^{-2}), and references
AlN	6.2	−0.081 (Andreev and O'Reilly 2001)
CdS hexagonal	2.4 E_g (A) 2.5 E_g (B) 2.55 E_g (C)	0.002 (Jerphagnon 1970)
CdS cubic	2.5	
CdSe hexagonal	1.75 E_g (A) 1.771 E_g (B) 2.17 E_g (C)	0.006 (Schmidt *et al* 1997, Hines and Guyot-Sionnest 1996)
CdSe cubic	1.9	
CdTe	1.49	de Paula *et al* (1998)
GaN	3.36	−0.029 (Zhang *et al* 1998, Micic *et al* 1999)
PbS	0.41	Nenadovic *et al* (1990), Machol *et al* (1993)
PbSe	0.27	Wehrenberg *et al* (2002)
TiO_2	3.2	Rajh *et al* (2004)
ZnS	3.68	Xu and Schoonen (2000)
ZnO	3.35	−0.07 (Jerphagnon 1970)

radii, it is possible to realize quantum dots that have emission spectra that peak at several selected wavelengths throughout the visible spectrum. Moreover, electrons in all of these quantum dots may be excited with a light source of one wavelength as long as the wavelength of the source is shorter than that of the emission wavelengths of all of the dots; accordingly, the simultaneous observation of multiple biological structures may be accomplished by labelling them with quantum dots of different colours and by pumping all of these quantum dots with the same source. This is in contrast with the situation encountered for fluorescent dyes, since each dye generally requires an excitation source of a well defined wavelength. Each of these different-coloured quantum dots may be functionalized with a unique ligand–biomolecule pair to facilitate binding to a particular biological structure. For example, yellow quantum dots functionalized with GGGLDV will have an affinity for binding to $\alpha_4\beta_1$ integrins, and red quantum dots functionalized with GGGDGEA will have an affinity for binding to $\alpha_2\beta_1$ integrins. By functionalizing the quantum dots with antibodies, it is possible to achieve very high binding affinities.

In biological applications, colloidal quantum dots offer significant advantages over other types of quantum dots such as those created by laser ablation or by self-assembly on a surface. Colloidal quantum dots may be synthesized through chemical means in water-based electrolytic suspensions at densities of approximately 10^{16} quantum dots cm^{-3} (Alexson *et al* 2004). Ligands and biomolecules introduced into these suspensions may be bound to these suspended quantum dots through chemical techniques such as the cross-linking and thiol-bonding techniques described previously. Table 1 identifies a number of quantum dots that may be synthesized in such water-based colloidal suspensions.

CdSe-based quantum dots are of special interest since it has been discovered (Hines and Guyot-Sionnest 1996) that a thin coating of ZnS on a 2.7–3.0 nm diameter CdSe quantum dot passivates the core CdSe quantum dot, with the result that high quantum yields of 50% are observed at room temperature; this ZnS coating was also found to improve the photochemical

stability of the quantum dot. Bruchez *et al* (1998) reported the synthesis and use of water-soluble QDs for biological applications using silane/silica coatings on CdSe–CdS core–shell quantum dots. This silane/silica coating layer is hydrophilic and contains functional groups for covalent conjugation. In the work of Bruchez *et al* (1998), green coloured nanocrystals coated with trimethoxysilylpropyl urea and acetate groups were observed to bind with high affinity in the cell nucleus and the avidin–biotin interaction, a model system for ligand–receptor binding, was used to specifically label the F-actin filaments. In separate work, Chan and Nie (1998) employed a procedure for preparing water-soluble and biocompatible QDs, based on the use of a bifunctional organic compound—mercaptoacetic acid. The mercapto group binds to a Zn atom when it reacts with the ZnS-capped CdSe quantum dots in chloroform. Moreover, the polar carboxylic acid group renders the quantum dots water soluble, and the carboxyl group may be used for covalent coupling to biomolecules by cross-linking to reactive amine groups. Moreover, CdSe–ZnS QDs were conjugated with transferrin—a protein that on binding to a transferrin receptor signals receptor-mediated transfer (endocytosis) of material from the extracellular region of the cell into the cell's interior cytoplasmic region—and then these transferrin–quantum dot bioconjugates were observed to be transported into the cytoplasm of the cells. When imaged with a fluorescence microscope, these quantum dots appear in clusters or aggregates that resemble the vesicles normally associated with endocytosis. In separate work, Mattoussi *et al* (2000) demonstrated the synthesis of CdSe–ZnS quantum dot bioconjugates using engineered recombinant proteins. In addition, Mattoussi *et al* (2000) developed a conjugation strategy, based on self-assembly utilizing electrostatic attractions between negatively charged dihydrolipoic acid (DHLA) capped CdSe–ZnS quantum dots and engineered bifunctional recombinant proteins consisting of positively charged attachment domains (containing a leucine zipper) genetically fused with desired biologically relevant domains, which could be achieved by using a naturally charged molecule, such as avidin, or a protein of interest fused to a positively charged leucine zipper peptide. The techniques introduced by Mattoussi *et al* (2000) further extend and complement the previously discussed methods for conjugating quantum dots and biomolecules. The functionalization of quantum dots with antibodies has been pursued by Wu *et al* (2003), who have made major demonstrations of the utility of using semiconductor quantum dots as fluorescent probes in the study of subcellular phenomena with nanoscale precision. In the work of Wu *et al* (2003), ZnS-coated CdSe semiconductor quantum dots functionalized with IgG antibody and streptavidin were used to label the breast cancer marker Her2 on the surfaces of both fixed and live cancer cells and other cellular targets like nuclear antigens inside cell nuclei, actin, and microtubules. Building on the earlier work of Mattoussi *et al* (2000), Jaiswal *et al* (2003) have used the technique of electrostatic self-assembled CdSe–ZnS quantum dots to accomplish long-term multiple-colour imaging of live cells for periods of over a week as the cells developed and grew; in this work, a synthetically engineered protein G-zb (leucine zipper-containing peptide fused to the B2 binding domain of streptococcal protein G) or avidin was used to conjugate antibodies to colloidal quantum dots. The noninvasive labelling of mammalian HeLa cells through endocytosis of DHLA-capped quantum dots was observed. Moreover, it appeared that in these studies the DHLA-capped QDs did not interfere with normal cellular functions such as endocytosis, motility, and cellular signalling. In particular, Jaiswal *et al* (2003) conclude that these approaches for noninvasive cell labelling are viable for periods of over12 days and that cell growth and motility are not affected. In yet another study, by Akerman *et al* (2002), tri-*n*-octylphosphine oxide-coated ZnS-capped CdSe QDs were synthesized and coated with mercaptoacetic acid to render them water-soluble. These quantum dots were coated with three peptides: CGFECVRQCPERC peptide (GFE peptide), which in lung blood vessels binds to the membrane dipeptidase on the endothelial cells in the

lung blood vessels; KDEPQRRSARLSAKPAPPKPEPKPKKAPAKK peptide (F3 peptide), which in various tumours preferentially binds to the blood vessels and tumour cells; and CGNKRTRGC (LyP-1), which in certain tumours recognizes the lymphatic vessels and the tumour cells. By injecting suspensions of these quantum dots into the blood stream of a mouse, it was verified that these peptide-functionalized quantum dots did indeed bind to the indicated biological structures. In another example, Dahan *et al* (2003) have used streptavidin-functionalized CdSe–ZnS QDs to track and image glycine receptor (GlyR) diffusion dynamics in a neuronal membrane for timescales varying from microseconds to minutes. In the study of Dahan *et al* (2003), the detection of endogenous GlyR α1 subunits at spinal cultured neuron surfaces was realized by using mAb2b primary antibody, biotinilated anti-mouse Fab fragments, and QDs emitting at 605 nm. By following the trajectories of QD-GlyR complexes, diffusion coefficients were obtained. Dahan *et al* (2003) found that the trajectories of QD-labelled GlyRs could be visualized for at least 20 min whereas those labelled with Cy3-dye-coupled antibody were visible for only 5 s, providing yet another example of the superior performance of quantum dots. In the work of Dahan *et al* (2003), it was found (1) that blinking of a single quantum dot provided a useful signature for tracking the movement of the dot through fluorescence microscopy and (2) that a lateral resolution with QDs of about 5–10 nm could be achieved while that with Cy3 was only about 40 nm.

Alexson *et al* (2004), Winter *et al* (2001) and Shi *et al* (2004) have conjugated CGGGRGD peptides to QDs, and then the QD–peptide complexes were used to target integrins spanning the membrane of a cell. As has been discussed previously, short peptides containing RGD and LDV bind to selected integrins. These investigators (Alexson *et al* 2004, Shi *et al* 2004) have conjugated different peptides containing motifs such as LDV and RGD to both CdS-mercaptoacetic (CdS/M) QDs and carboxylic-group-functionalized CdSe–ZnS QDs. As for the CdS/M colloidal dots synthesized at the University of Illinois at Chicago in our research group, the cysteine (C) amino acid on one end of the peptides—CGGGRGDS and CGGGLDV—is provided for binding to semiconductor nanocrystals through the relatively strong thiol linkage; on the other hand, CdSe–ZnS quantum dots with a coating containing carboxylic terminal groups from Evident Technologies were conjugated with peptides—GGGGRGDS and GGGGLDV—through simple covalent bonding by using a common cross-linking reagent—EDC (1-ethyl-3-(3-dimethylamino propyl) carbodiimide). The glycine (G) amino acids, with a simple hydrogen side group, served as spacing elements. Accordingly, glycine is a natural choice for the bridging amino acid between the C terminus amino acids as a result of the simple side group of a single hydrogen atom that should produce minimal packing effects. These conjugates are used to tag the HT1080 human fibrosarcoma cells that are observed under a fluorescent microscope. CdS quantum dots were synthesized by using a previously published method (Chen *et al* 2000). In short, CdS nanocrystals were prepared by arrested precipitation at room temperature in an aqueous solution using mercaptoacetic acid as the colloidal stabilizer. Reagents were purchased from Sigma. Specifically, 36.6 mg of $CdCl_2$ was diluted in DI water, resulting in 40 ml of a 5 mM solution. This solution was titrated with mercaptoacetic acid to pH 2, resulting in a turbid blue solution. The pH value was then raised to 7 with concentrated NaOH and the solution turned colourless once again. While stirring the solution, 40 ml of 5 mM $Na_2S{\cdot}9H_2O$ was added to the mixture and the solution turned yellow in a few minutes, indicating the formation of CdS/M clusters (about 2.5 mM). These CdS/M quantum dots were functionalized with peptides by adding peptides CGGGRGDS or CGGGLDV directly to the final solution, and incubating overnight. The ratio of peptide versus quantum dots was determined through simple calculation. Chan *et al* (2002) claim that two to five normal-sized protein molecules and 50 or more small molecules like peptides may be conjugated to a single 4 nm QD. Accordingly, the molar ratio of peptides to quantum dots

was taken as 50:1. Though quantum dots are sometimes observed to form large clusters, there are about 10^{16} dots cm^{-3} in the final solution, and the corresponding peptide density is approximately 1 mg ml^{-1}. Another type of quantum dot investigation in this research is the ZnS-capped CdSe dot, which is known to have a high quantum yield of about 50%. The water-soluble CdSe–ZnS dots coated with carboxylic terminal groups were obtained from Evident Technologies. As a result of the carboxyl group on the surface of these dots, they may be coupled to proteins and antibodies containing active amine groups by using the EDC cross-linking procedure described previously. Quantum dots of two different colours are used: one with an emission peak at 605 ± 10 nm, which is conjugated with GGGGRGDS; and another with an emission peak at 565 ± 10 nm, which is conjugated with GGGGLDV. Other chemicals, including EDC, sulfo-NHS, MES, and boric acid, were purchased from Sigma. The binding of peptides to the surface of quantum dots was accomplished by using a modified version of previously reported methods (Hermanson 1996); 5 mg EDC, 3.75 mg sulfo-NHS, 0.2 ml MES buffer (0.1 M MES, pH 6.0) and 0.3 ml DI water were added to 0.5 ml carboxyl-QDs (4 nmol ml^{-1} for QDs emitting at 565 nm and 2 nmol ml^{-1} for QDs emitting at 605 nm), stirred and allowed to react for 30 min. The next step was to centrifuge at 4000 rpm for 40 min and discard the supernatant in order to remove extra chemicals. Then, the pellets were rinsed gently twice with 1 ml of DI water. The following were then added to the precipitate: 0.5 ml peptide solution (1 mg ml^{-1}), 0.3 ml DI water, and 0.2 ml sodium borate buffer (pH 8.3 0.1 M boric acid); then the pellet was (1) incubated in a ultrasonic bath until it dissolved, (2) allowed to react for two hours, and (3) stored at 4 °C overnight. The excess of peptide and by-products of the reaction were removed by several rounds of centrifugation. The resulting concentration is about 2 nmol ml^{-1} for QDs emitting at 565 nm and 1 nmol ml^{-1} for QDs emitting at 605 nm.

The bandgap of bulk CdS at 10 K is 2.58 eV (480.6 nm) and the bandgap increases to approximately 2.8 eV (439.9 nm) for a 3 nm diameter CdS quantum dot as a result of the quantum confinement (Chen *et al* 2000, Winter *et al* 2001, Alexson *et al* 2004). The absorption spectra of CdS/M quantum dots alone and CdS/M quantum-dot–peptide complexes were measured by a Beckman Coulter DU-640 spectrophotometer. The PL spectra of CdS QDs were obtained using a 514 nm Ar laser source to ensure the sub-bandgap excitation of the CdS–peptide complexes. The carboxyl–CdSe–ZnS QDs, purchased from a commercial source (Evident Technology), have well defined optical properties. To determine whether the peptide conjugation has any effects on the optical properties of the original quantum dots, absorption spectra of dots before and after peptide conjugation were taken by using a Beckman Coulter DU-640 spectrophotometer. The cells used in one portion of this study were HT1080 fibrosarcoma cells; these were cultured in medium consisting of Dulbecco's modified Eagle's medium (DMEM) with 1000 mg l^{-1} glucose, L-glutamine and sodium bicarbonate, 10% foetal bovine serum, and 10 unit ml^{-1} penicillin. Cells were grown on a 22 mm × 22 mm coverslip, which was maintained in a Petri dish. At first, the cells were supplied with 0.5 ml medium and kept in a incubator with 5% CO_2 at 37 °C for 1 h in order to allow the cells to attach to the surface of the coverslip, and then 2 ml medium was added to the Petri dish and incubated overnight for the cells to spread completely over the coverslip. As mentioned previously, RGD- or LDV-based peptides were selected in this research. This selection was based on a reported analysis of integrin expression pattern on HT1080 fibrosarcoma cells. By using antibodies directed against integrins and integrin subunits, Schifferli and Henrich (1996) show that different types of integrins including $\alpha_2\beta_1$, $\alpha_3\beta_1$, and $\alpha_5\beta_1$ were expressed on HT1080 cells.

As described previously, both LDV and RGD bind to $\alpha_5\beta_1$, and RGD binds to $\alpha_3\beta_1$ as well. QD–peptide complexes were bound to cells using standard immunocytology techniques (Javois 1999). In short, cells were taken out from the incubator and gently washed with

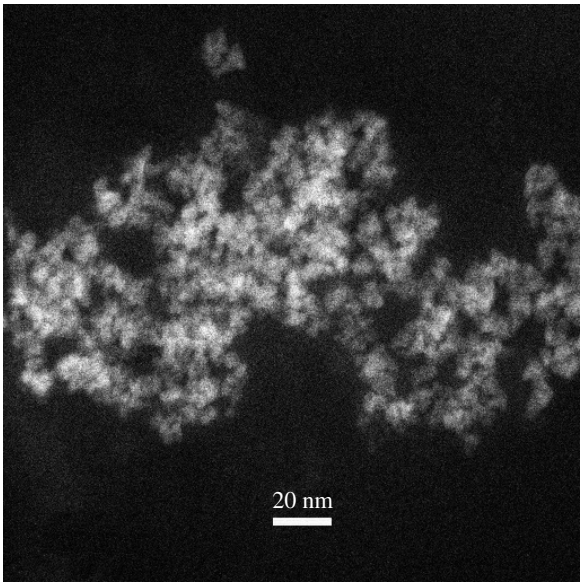

Figure 4. TEM image of a CdS/M QD sample.

PBS (pH 7.4, Sigma) three times. Then the following steps were taken: block the cells with PBS + 2% BSA for 30 min; remove the blocking solution and wash with PBS three times; for a 38 mm Petri-dish, add 1–2 ml 3.7% formaldehyde; wait for 15 min to fix the cells; remove fixing solution and wash with PBS three times. The cells were then ready for staining. The final QD–peptide solution used for labelling cells was highly diluted with PBS to a concentration of approximately 15–20 nM to prevent the cells from being subjected to an excessive density of quantum dots. For each sample, the following operations were performed: 1 ml diluted conjugate solution was added; the solution was allowed to cover the whole coverslip evenly for 10 min; then the coverslips were washed with PBS thoroughly to remove the extra quantum dots. Next, the coverslip was mounted on a glass slide upside down (the surface with cells faced the glass slide) for observation. PBS was added in the space between the coverslip and glass slide, so that the cells would not dry out. The samples were imaged using a Nikon Eclipse E800 fluorescent microscope with a 100× oil immersion objective (NA 1.40). Different filter sets (purchased from Chroma Technology) were used for each kind of dot: for the CdS/M dots, the excitation light is centred at 360 ± 40 nm and a low pass emission filter is used for signal collection; for the CdSe–ZnS quantum dots, the excitation light spans from UV to blue, and emission filters centred at 605 ± 20 nm and 565 ± 20 nm were used for the previously described quantum dots.

The self-made CdS/M solution was observed by scanning transmission electron microscope (TEM, Research Resources Centre at UIC). Figure 4 is a typical TEM micrograph showing the morphology and size of CdS/M QDs. The QDs appear to cluster together as in figure 4. This clustering is expected when the water is evaporated, since the QDs then attract each other through the van der Waals force.

Careful analysis of the image reveals that the CdS/M cluster consists of many small globular CdS particles with a diameter of about 3 nm, which dictates the optical properties of the CdS/M quantum dots.

The previously calculated absorption peak (439.9 nm) may be compared with and confirmed from absorption spectrum measurement as shown in figure 5. The absorption peak

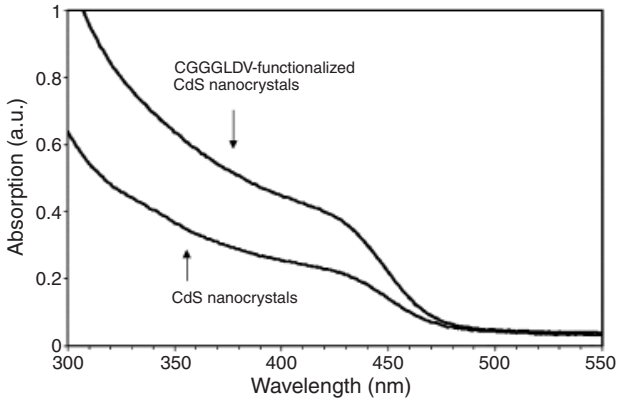

Figure 5. Absorption spectrum of CdS/M and LDV functionalized CdS/M QD suspension.

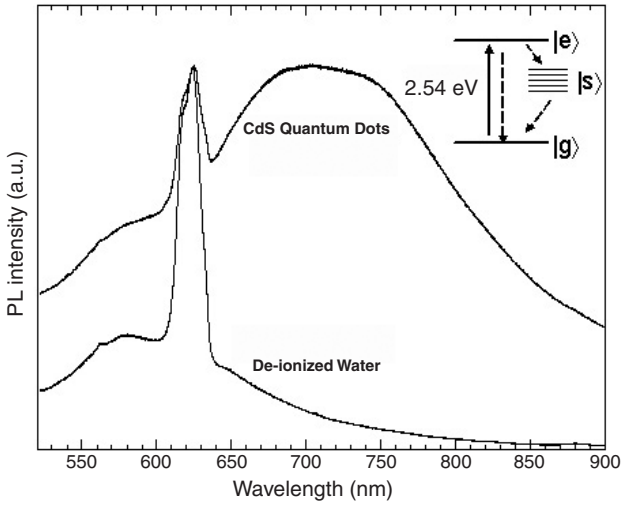

Figure 6. PL spectrum of CdS/M QDs. The upright diagram illustrates the process of surface state emission.

corresponding to the transition between the lowest state in the conduction band and the highest state in the valence band is around 440 nm. In CdS nanocrystals, the quantum confinement effects dominate over both the excitonic binding energy of about 30 meV and the effects of relatively weak spontaneous polarization (Alexson *et al* 2004).

As shown in the PL spectrum of figure 6, a strong PL feature due to the recombination of the electron–hole pair at the quantum confined state is not present, while the dominant feature of photoluminescence found around 700 nm is due to the recombination from surface states in the bandgap of the semiconductor, which is most likely caused by surface traps as is illustrated in figure 6. These states do not exist in the ZnS-capped CdSe QDs. The peak near 620 nm is due to the presence of DI water or glass tube. The QDs conjugated with peptides exhibit PL spectra identical to those of QDs without peptide coating.

To determine whether the conjugation of peptides has any effects on the optical properties of the carboxyl–CdSe–ZnS dots, absorption spectra before and after attachment of peptides were measured; based on these results, it appears that attaching the peptide to the surface of

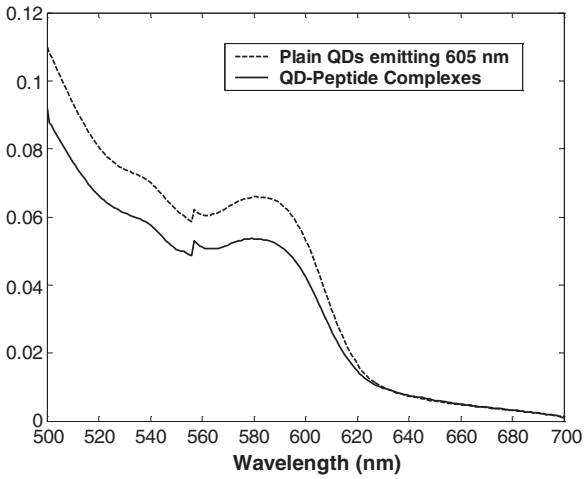

Figure 7. Absorption spectra of CdSe–ZnS QDs with an emission spectrum of 605 nm before and after conjugation with peptide GGGGRGDS.

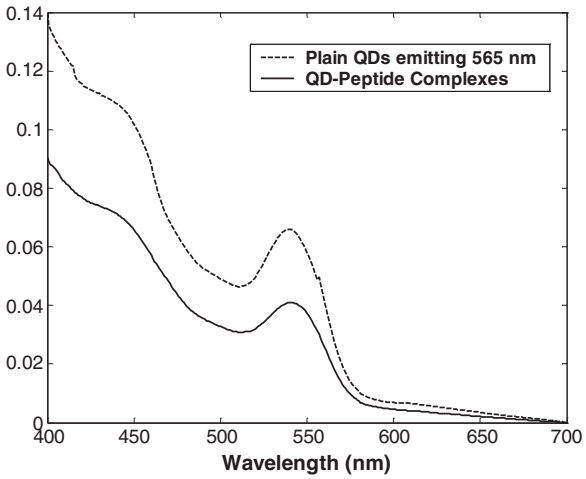

Figure 8. Absorption spectra of hops of yellow CdSe–ZnS QDs before and after conjugation with peptide GGGGLDV.

the QDs does not affect the absorption spectra of the dots significantly, as shown in figures 7 and 8; a distinct absorption peak of the same wavelength is observed.

Figure 9 shows the results of successful labelling of HT1080 human fibrosarcoma cells with the CdS/M QD–peptide (CGGGLDV) complexes. The bright dots around the edge of the cell in part (B) of figure 9 are fluorescence from the CdS/M QDs clusters and the dim area in the cell body is auto-fluorescent due to the near UV excitation.

In an example of LDV-directed labelling, the peptide GGGGLDV was conjugated with CdSe–ZnS QDs emitting at 600 ± 10 nm. Figure 10 shows the results of labelling cells with the conjugates. As previously described, the RGD containing peptide sequence can mimic the adherent ligand for almost half of the entire family of integrins. So even though the final solution of QD–peptide complexes used for tagging was only 15 nmol l^{-1}, fluorescent dots

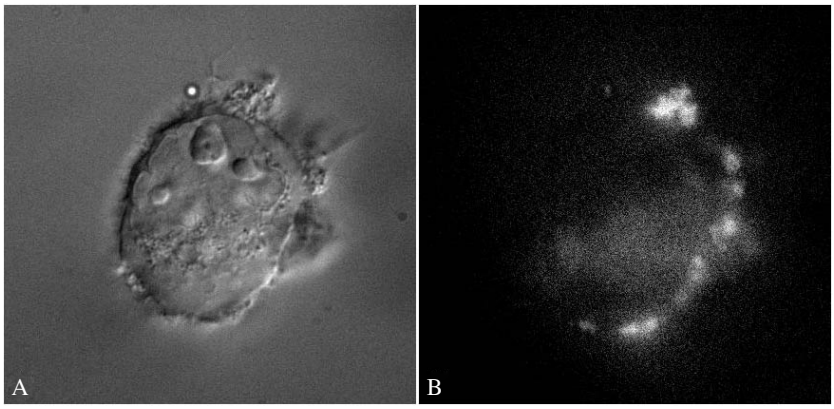

Figure 9. CdS/M QD–peptide (CGGGLDV) complexes binding to cells. (A) Bright-field image of HT1080 cells. (B) The same cell labelled with CdS/M QD–peptide complexes.

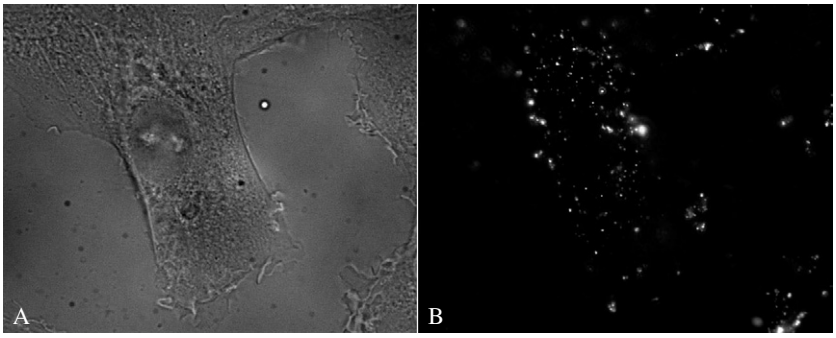

Figure 10. Peptide (GGGGRGDS) conjugated with CdSe–ZnS QDs (565 nm emission) bound to cells. (A) Bright-field image of HT1080 cells. (B) The same cell labelled with QD–peptide complexes.

are bound at many locations distributed over the surface of the cell as shown in part (B) of figure 10, which reflects the expression pattern of RGD receptors over the cells.

In order to study the incorporation of quantum dots into the internal cytoplasm of a cell, CdSe–ZnS QDs were functionalized with transferrin using the techniques of Chan and Nie (1998). The transferrin was bound to carboxyl-functionalized CdSe–ZnS quantum dots using the EDC crossing-linking procedure. Equal masses of transferrin and quantum dots were used. Using the previously described techniques, HeLa cells were incubated with these transferrin-functionalized quantum dots at a concentration of 30 nM. Figure 11 presents a fluorescence image of HeLa cells that were incubated with transferrin-functionalized CdSe–ZnS quantum dots for 1 h. The images of figure 11 reveal that quantum dots were inside or on the surface of the cell.

Figure 12 depicts HeLa cells that have been incubated for 3 h with transferrin-functionalized CdSe–ZnS QDs at a concentration of 30 nM. With increase in incubation time, a large number of quantum dots have entered the cell by the process of receptor-mediated endocytosis; the receptors on the cell surface appear to have been recognized by the transferrin molecules.

Rajh and co-workers (Paunesku *et al* 2003, Rajh *et al* 1999, 2002, 2004) have investigated a nanocomposite system by covalently bonding nanoparticles of titanium dioxide (TiO_2) to

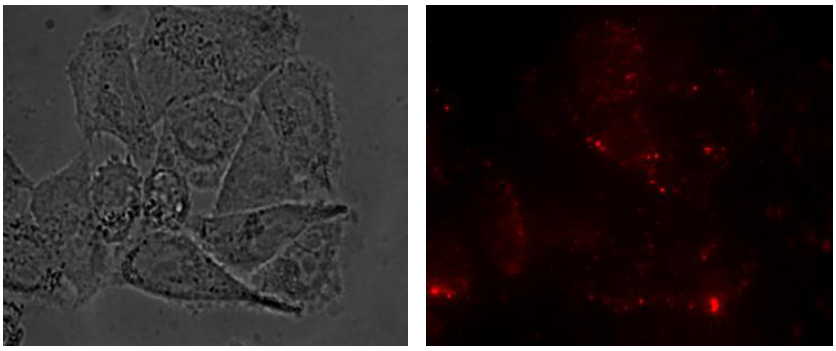

Figure 11. HeLa cells incubated with transferrin conjugated CdSe–ZnS quantum dot (565 nm emission) at 30 nM concentration for 1 h. Bright-field image at 100× (left). Fluorescence image at 100× (right).

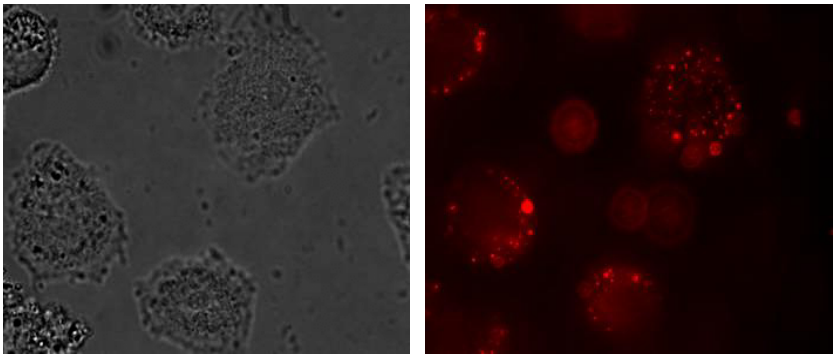

Figure 12. HeLa cells incubated with transferrin-conjugated CdSe–ZnS QDs at a concentration of 30 nM for three hours. Bright-field image of cell at 100× (left). Bright-field image superimposed on the fluorescence image at 100× (right).

oligonucleotide DNA. Unlike the other semiconductor nanocrystals considered in this paper, titanium dioxide is not a direct bandgap semiconductor. Rajh and co-workers (Paunesku *et al* 2003, Rajh *et al* 1999, 2002, 2004) demonstrated that these nanocomposites retain the intrinsic photocatalytic capacity of titanium dioxide and the bioreactivity of oligonucleotide DNA; however, these nanocomposites also possess the biologically and chemically unique property of a light-inducible nucleic acid endonuclease, which could provide a new means of using nanocomposites and photon-excited transitions in semiconductor nanoparticles for gene therapy. These results indicate that integrated complexes of manmade nanoscale semiconductors and biomolecules hold the promise of providing new means of altering and controlling intracellular manipulation. Specifically, these approaches provide the means of creating of chemical–biological hybrid nanocomposites that can be introduced into cells and subsequently used to initiate intracellular processes or biochemical reactions. Indeed, Rajh *et al* (2004) show that photoresponsive inorganic nanoparticles serve as a source of photogenerated charges that act as reporters of the electronic properties of biomolecules. Rajh and co-workers (Paunesku *et al* 2003, Rajh *et al* 1999, 2002, 2004) have shown that photoactive bioorganic TiO_2/dopamine/DNA triads are capable of light induced manipulation of biomolecules such as cleavage of the DNA at GG sites by radical cations (holes) that are created by light in the TiO_2/dopamine complex and that then propagate along the DNA to

GG sites when they cause cleavage of the DNA. Moreover, Rajh *et al* (2004) show that using bridging ligands such as dopamine (DA) facilitate hole transfer across the interface between the TiO_2–DNA. Rajh and co-workers (Paunesku *et al* 2003, Rajh *et al* 1999, 2002, 2004) demonstrated further that bioinorganic triads such as TiO_2–DA–DNA are capable of complex photo-chemistries such as light-induced manipulation of biomolecules and their switching functions. These results portend applications of oligonucleotide–TiO_2 nanocomposites in photoinduced endonuclease activity. Paunesku *et al* (2003) have verified through the use of gel electrophoresis that cleavage of DNA at G-rich sites occurs in accord with the expected bond breaking caused by holes produced by photoexcitation of electron–hole pairs in the TiO_2 bound to the DNA. Additional insights into the findings of Rajh *et al* (2004) and Schuster (2000) are given by recent theoretical efforts aimed at understanding charge transport in DNA. Specifically, Conwell and Rakhmanova (2000) have modelled hole transport in DNA using the Su–Schrieffer–Heeger Hamiltonian (Su *et al* 1980) and suggest that hole mobility in DNA is due to polaron drift similar to that in chains of conjugated polymers. Conwell and Rakhmanova (2000) and Rakhmanova and Conwell (2001) construct and adapt a set of parameters for a Su–Schrieffer–Heeger Hamiltonian appropriate to DNA and they present a model for a band structure of DNA based on a spreading of the HOMO levels for a series of cytosine/guanine and adenine/thymine bases. Conwell and Rakhmanova (2000) estimate that the hole energy is reduced by 0.25 eV due to polaron formation, and estimate the transfer integral, the hole–phonon interaction coefficient, zone-edge phonon energy ($\pi v_{\mathrm{sound}}/a$), and elastic constant to be 0.36 eV, 6 eV nm^{-1}, 34 THz, and 8.5 eV nm^{-1}, respectively. In addition, Conwell and Rakhmanova (2000) predict that the polaron is about five to seven base pairs wide, depending on the base sequence. These findings are supportive of the conceptual models advanced by Schuster (2000). Moreover, Rakhmanova and Conwell (2001) have extended their previous model (Conwell and Rakhmanova 2000) of hole drift in DNA by inclusion of an electric field in the Su–Schrieffer–Heeger Hamiltonian. Rakhmanova and Conwell (2001) find that for a field of 5.8×10^3 V cm^{-1} the polaron moves 7 bases, or 2.4 nm, in 138 ps. For DNA with random G/C (guanine/cytosine) and A/T (adenine/thymine) base sequences, the centre of the polaron was found to hop on a picosecond timescale between guanines or between a guanine and an adenine, separated by up to a few bases.

4. Semiconducting and metallic carbon nanotubes in biological applications

The interfacing of carbon-nanotube-based nanowires directly with active biological structures, including neurons, is potentially leading to a way of monitoring and controlling bioelectronic signals. Indeed, Li *et al* (2003) have used a carbon-nanotube nanoelectronic array for ultrasensitive DNA detection. The development of carbon-nanotube (CNT) transistors represents another step in the technology development of CNT-based devices and structures that portend biological applications (Shim *et al* 2002, 2001, Siddons *et al* 2004). In separate work, Wong *et al* (1998) have developed covalently functionalized nanotubes as nanometre-sized probes for biological applications.

Of potential importance to future directions in the integration of CNT-based devices with biological structures are the current advances in the integration of manmade nanostructures having both optical and electronic components (Ravindan *et al* 2003); in particular, these authors report on the synthesis of multiwalled carbon-nanotube–quantum dot heterojunctions using the ethylene carbodiimide coupling procedure. The ability to functionalize nanostructures in aqueous environments so that they have binding affinities to neurons (Stroscio and Dutta 2004) points the way to making massively parallel electrical CNT-based nanowire interconnects to neurons through the use of chemically directed assembly.

Indeed, the use of CNTs as nanowires has been investigated by a growing number of investigators (Stroscio and Dutta 2004, Shim *et al* 2002, Sethuraman *et al* 2004).

As discussed by Sethuraman *et al* (2004), carbon nanotubes (CNTs) portend many applications in bioelectronics and in the field of biomedical engineering as a result of their nanoscale diameters and as a result of the fact that they may be produced as metallic or semiconducting nanostructures. In addition, Lu and Han (1998) have discussed the general properties and uses of carbon nanotubes and nanotube-based nano devices. Of special significance in the context of the electrolytic environments that are pervasive in biological structures, Kruger *et al* (2001) have explored the electric-field effect of carbon nanotubes in electrolytes; they find that as a result of the large gate capacitance Fermi energy (E_F) shifts of order of a volt may be induced. Consequently, this electrolytic tuning makes it possible to tune CNTs from n- to p-type. Kruger *et al* show that at zero gate voltage the CNTs are hole-doped in air with $|E_F| \approx 0.3$–0.5 eV, corresponding to a doping level of $\approx 10^{13}$ cm^{-2}. In separate work, Kavan *et al* (2001) have shown that the population of valence band electronic states of single-walled carbon nanotubes (SWNTs) may be tuned electrochemically in acetonitrile electrolyte solution.

The design and fabrication of CNT-based transistors (Collins and Avouris 2002, Collins *et al* 2001, Javey *et al* 2004a, 2004b) has advanced greatly in recent years and the carrier transport in CNTs has been described as quasi-ballistic (Javey *et al* 2004a). The transport of carriers in CNTs is known to be limited by the scattering of carriers from phonons (Raichura *et al* 2004a, 2004b, Stroscio and Dutta 2001). Moreover, Raichura *et al* (2004b) have recently shown that it is important to consider dimensional confinement effects in modelling the influence of carrier–phonon scattering in charge transport and mobility in CNTs. Indeed, Raichura *et al* (2003) have identified a number of phonon modes in CNTs that contribute to the full set of vibrational modes of SWNTs, and Raichura *et al* (2004b) have shown that phonon bottleneck effects are important in modelling charge transport in CNTs. Based on these results, the carrier transport properties—including carrier mobility—of CNTs are well suited for biological applications.

In an important example of the functionalization of the walls of CNTs by peptides and other chemical agents so that they bind selectively to biological structures, single-walled carbon-nanotube-based electronic biomolecular probes of Shim *et al* (2002) have significant potential for the study of critically important transmembrane proteins including integrins, receptors, and ion channels. Motivated by the need for biocompatibility of such CNT-based structures, Shim *et al* (2002) have shown that functionalization of the nanotube surface by a coabsorption of Triton and poly(ethylene glycol) (PEG) is effective in making the nanotube resistant to nonspecific absorption of streptavidin. As a result of their environment-sensitive electrical conductivity, single-walled carbon nanotubes (SWNTs) may be well suited for sensor applications in biological environments. Indeed, this sensitivity has been exploited (Shim *et al* 2002, 2001, Siddons *et al* 2004) in the development of SWNT field-effect transistors (FETs). SWNT FETs generally exhibit p-type conduction; however, Shim *et al* (Shim *et al* 2002, 2001, Siddons *et al* 2004) have shown that polymers with amine groups such as polyethylenimine can convert the p-type device into an n-FET whereas poly(ethylene oxide) leads to ambipolar characteristics.

5. Conclusions

The exploitation of semiconductor nanostructures in biological applications has advanced dramatically in the last half decade. For the first time, different peptide sequences were selected as the recognition molecules and conjugated with different kinds of QDs through

distinct schemes. Also demonstrated is integrin-selective binding of QD–peptide complexes to integrins of numerous types of cells. Moreover, QD–antibody complexes have been shown to bind to biological structures—including biomolecules—with high specificity. These nanoscale semiconductor tags have been used to study the dynamics of biological processes including those of neuronal processes. Semiconductor QDs have shown great advantages in ultrasensitive immunofluorescence monitoring of long term cellular processes such as protein movement under different conditions and message signalling. The length of a peptide varies according to the number of amino acids, since each amino acid has a length of about 3 Å. This provides nanometre-scale control over the separation distance between the QDs and the cell. Such a capability is essential to the investigation of the interaction of QDs with biological structures. Moreover, selected semiconductor nanocrystals have very strong dipole moment due to spontaneous polarizations up to about 0.1 C m^{-2}, which may elicit ion channel turn-on and turn-off. In recent years, semiconductor quantum dots have been bound to duplex DNA and have been used as optically stimulated electrical interfaces that inject carriers into DNA and provide a means of engineering the DNA through processes such as site selective strand cleavage. Finally, techniques required to use carbon nanotubes as nanowire interconnects with selected biological structures are being developed.

Acknowledgments

This work was supported by ARO under the direction of Dr Dwight Woolard, by AFOSR under the direction of Dr Todd Steiner, and by an AFOSR DURIP.

References

Akerman M E, Chan W C, Laakkonen P, Bhatia S N and Ruoslahti E 2002 Nanocrystal targeting *in vivo Proc. Natl Acad. Sci. USA* **99** 12617

Alberts B, Johnson A, Lewis J, Raff M, Roberts K and Walter P 2002 *Molecular Biology of the Cell* 4th edn (New York: Garland Science)

Alexson D, Li Y, Ramadurai D, Shi P, George L, Uddin M, Thomas P, Rufo S, Dutta M and Stroscio M A 2004 Binding of semiconductor quantum dots to cellular integrins *IEEE Trans. Nanotechnol.* **3** 86

Alivisatos A P 1996 Perspectives on the physical chemistry of semiconductor nanocrystals *J. Phys. Chem.* **100** 13226

Andreev A D and O'Reilly E P 2001 Theory of the electric structure of GaN/AlN hexagonal quantum dots *Phys. Rev.* B **62** 15851

Banyai L and Koch S W 1993 *Semiconductor Quantum Dots* (Singapore: World Scientific)

Bruchez M Jr, Moronne M, Gin P, Weiss S and Alivisatos A P 1998 Semiconductor nanocrystals as fluorescent biological labels *Science* **281** 2013

Chan W C, Maxwell D J, Gao X, Bailey R E, Han M and Nie S 2002 Luminescent quantum dots for multiplexed biological detection and imaging *Curr. Opin. Biotechnol.* **13** 40

Chan W C and Nie S 1998 Quantum dot bioconjugates for ultrasensitive nonisotropic detection *Science* **281** 2016

Chen C, Dutta M and Stroscio M A 2004 Surface-optical phonon assisted transitions in quantum dots *J. Appl. Phys.* **96** 2049

Chen H M, Huang X F, Xu L, Chen K J and Feng D 2000 Self-assembly and photoluminescence of CdS-mercaptoacetic clusters with internal structures *Superlatt. Microstruct.* **27** 1

Chen R, Zhang Y, Wang D and Dai H 2001 Noncovalent sidewall functionalization of single-walled carbon nanotubes for protein immobilization *J. Am. Chem. Soc.* **123** 3838

Collins P G, Arnold M S and Avouris P 2001 Engineering carbon nanotubes and nanotube circuits using electrical breakdown *Science* **292** 706

Collins P G and Avouris P 2002 Multishell conduction in multiwalled carbon nanotubes *Appl. Phys.* A **74** 1

Conwell E M and Rakhmanova S V 2000 Polarons in DNA *Proc. Natl Acad. Sci. USA* **97** 4556

Dahan M, Levi S, Luccardini C, Rostaing P, Riveau B and Triller A 2003 Diffusion dynamics of glycine receptors revealed by single quantum dot tracking *Science* **302** 442

de Paula A M, Barbosa L C, Cruz C H B, Alves O L, Sanjurjo J A and Cesar C L 1998 Quantum confinement effects on the optical phonons of CdTe quantum dots *Superlatt. Microstruct.* **23** 1104

Empedocles E, Norris D J and Bawendi M G 1996 Photoluminescence spectroscopy of single CdSe nanocrystallite quantum dots *Phys. Rev. Lett.* **77** 3873

Hermanson G T 1996 *Bioconjugate Techniques* (San Diego, CA: Academic)

Hines M and Guyot-Sionnest P 1996 Synthesis and characterization of strongly luminescing ZnS-capped CdSe nanocrystals *J. Phys. Chem.* **100** 468

Hynes R O 1992 Integrins: versatility, modulation, and signaling in cell adhesion *Cell* **69** 11

Jaiswal J K, Mattoussi H, Mauro J M and Simon S M 2003 Long-term multiple-color imaging of live cells using quantum dot bioconjugates *Nat. Biotechnol.* **21** 47

Javey A, Guo J, Paulsson M, Wang Q, Mann D, Lundstrom M and Dai H 2004a High field quasi-ballistic transport in short carbon nanotubes *Phys. Rev. Lett.* **92** 106804

Javey A, Guo J, Wang Q, Lundstrom M and Dai H 2004b Ballistic carbon nanotube field-effect transistors *Nature* **424** 654

Javois L C 1999 *Immunocytochemical Methods and Protocols* 2nd edn (Totowa, NJ: Humana Press)

Jerphagnon J 1970 Imvariants of the third-rank Cartesian-tensor: optical nonlinear susceptibilities *Phys. Rev.* B **2** 1091

Jovin T M 2003 Quantum dots finally come of age *Nat. Biotechnol.* **21** 32

Kasten F H 1999 Introduction to fluorescent probes: properties, history and application *Fluorescent and Luminescent Probes for Biological Activity* 2nd edn, ed W T Mason (San Diego, CA: Academic) pp 17–38

Kavan L, Rapta P, Dunsch L, Bronikowski M J, Willis P and Smalley R E 2001 Electrochemical tuning of electronic structure of single walled carbon nanotubes: *in-situ* Raman and vis-NIR study *J. Phys. Chem.* B **105** 10764

Klarreich E 2001 Biologists join the dots *Nature* **413** 450–2

Kruger M, Buitelaar M R, Nussbaumer T, Schonenberger C and Forro L 2001 Electrochemical carbon nanotube field-effect transistor *Appl. Phys. Lett.* **78** 1291

Kuno M, Fromm D P, Hamann H F, Gallagher A and Nesbitt D J 2000 Nonexponential blinking kinetics of single CdSe quantum dots: a universal power law behavior *J. Chem. Phys.* **112** 3117

Li J L, Ng H T, Cassell A, Fan W, Chan H, Ye Q, Koehne J, Han J and Thurnauer M C 2003 Carbon nanotube nanoelectronic array for ultrasensitive DNA detection *Nano Lett.* **3** 597

Liboff R 1980 *Introductory Quantum Mechanics* (San Francisco, CA: Holden-Day)

Lu J P and Han J 1998 Carbon nanotubes and nanotube-based nano devices *Quantum-Based Electronic Devices and Systems* ed M Dutta and M A Stroscio (Singapore: World Scientific) pp 101–23

Machol J L, Wise F W, Patel R C and Tanner D B 1993 Vibronic quantum beats in PbS microcrystals *Phys. Rev.* B **48** 2819

Mattoussi H, Mauro J M, Goldman E R, Anderson G P, Sundar V C, Mikulec F V and Bawendi M G 2000 Self-assembly of CdSe–ZnS quantum dot bioconjugates using an engineered recombinant protein *J. Am. Chem. Soc.* **122** 12142

Micic O I, Ahrenkiel S P, Bertram D and Nozik A J 1999 Synthesis, structure, and optical properties of colloidal GaN quantum dots *Appl. Phys. Lett.* **75** 47

Mizejewski G J 1999 Role of integrins in cancer: survey of expression pattern *Exp. Bio. Med.* **222** 124

Nenadovic M T, Comor M I, Vasic V and Micic O I 1990 Transient bleaching of small PbS colloids *J. Phys. Chem.* **94** 6390

Paunesku T, Rajh T, Wiederrecht G, Maser J, Vogt S, Stojicevic N, Protic M, Lai B, Oryhon J, Thurnauer M and Woloschak G 2003 Biology of TiO_2–oligonucleotide nanocomposites *Nat. Mater.* **2** 343

Powell S K and Kleinman H 1997 Neuronal laminins and their cellular receptors *Int. J. Biochem. Cell. Biol.* **29** 401

Raichura A, Dutta M and Stroscio M A 2003 Deformation potential and acoustic phonon modes for single-wall carbon nanotubes of finite length *J. Appl. Phys.* **94** 4060

Raichura A, Dutta M and Stroscio M A 2004a Quantized optical vibrational modes of finite-length multi wall nanotubes: optical deformation potential *Superlatt. Microstruct.* **35** 147

Raichura A, Dutta M and Stroscio M A 2004b Continuum model for acoustic phonons in nanotubes: phonon bottleneck *Phys. Status Solidi* b **241** 3448

Rajh T, Chen L X, Lukas K, Liu M T, Thurnauer M C and Tiede D M 2002 Surface restructuring of nanoparticles: an efficient route for ligand-metal oxide crosstalk *J. Phys. Chem.* B **106** 10543

Rajh T, Nedeljkovic J M, Chen L X, Poluektov O and Thurnauer M C 1999 Improving optical and charge separation properties of nanocrystal TiO_2 by surface modification with vitamin C *J. Phys. Chem.* B **103** 515

Rajh T, Saponjic Z, Liu J, Dimitrijevic N M, Scherer N F, Vega-Arroyo M, Zapol P, Curtiss L A and Thurnauer M C 2004 Charge transfer across the nanocrystal-DNA interface: probing DNA recognition *Nano Lett.* **4** 1017

Rakhmanova S V and Conwell E M 2001 Polarons motion in DNA *J. Phys. Chem.* **105** 2056

Ravindan S, Chaudhary S, Colburn B, Ozkan M and Ozkan C S 2003 Covalent coupling of quantum dots to multiwalled carbon nanotubes for electronic device applications *Nano Lett.* **3** 447

Ruoslahti E 1996 RGD and other recognition sequences for integrins *Annu. Rev. Cell Dev. Biol.* **12** 697

Schifferli K P and Henrich C J 1996 Analysis of integrin expression and function in HT1080 cells using inhibitory anti-integrin antibodies *Focus* **18** 13

Schmidt M E, Blanton S A, Hines M A and Guyot-Sionnest P 1997 Polar CdSe nanocrystals: implications for electronic structure *J. Chem. Phys.* **106** 5254

Schuster G B 2000 Long-range charge transfer in DNA: transient structural distortions control the distance dependence *Acc. Chem. Res.* **33** 253

Sethuraman A, Stroscio M A and Dutta M 2004 Potential applications of carbon nanotubes in bioengineering *Biological Nanostructures and Applications of Nanostructures in Biology: Electrical, Mechanical and Optical* (*Bioelectric Engineering* vol 51) ed M A Stroscio and M Dutta (New York: Kluwer–Academic)

Shi P, Chen H, Cho M and Stroscio M A 2004 private communication

Shim M, Javey A, Kam N W S, Chen R J and Dai H 2002 Functionalization of carbon nanotubes for biocompatibility and bio-molecular recognition *Nano Lett.* **2** 285

Shim M, Javey A, Kam N W S and Dai H 2001 Polyners functionalization for air-stable n-type carbon nanotube field-effect transistors *J. Am. Chem. Soc.* **123** 11512

Siddons G P, Merchin D, Back J H, Jeong J K and Shim M 2004 Highly efficient gating and doping of carbon nanotubes with polymer electrolytes *Nano Lett.* **4** 927

Stroscio M A and Dutta M 2001 *Phonons in Nanostructures* (Cambridge: Cambridge University Press)

Stroscio M A and Dutta M (ed) 2004 *Biological Nanostructures and Applications of Nanostructures in Biology: Electrical Mechanical and Optical Properties* (New York: Kluwer–Academic)

Su W P, Schrieffer J R and Heeger A J 1980 Soliton excitations in polyacetylene *Phys. Rev.* B **22** 2099

Wehrenberg B L, Wang C and Guyot-Sionnest P 2002 Interband and intraband optical studies of PbSe colloidal quantum dots *J. Phys. Chem.* B **106** 10634

Winter J O, Liu T Y, Korgel B A and Schmidt C E 2001 Recognition molecule directed interfacing between semiconductor quantum dots and nerve cells *Adv. Mater.* **13** 1673

Wong S S, Joselevich E, Woolley A T, Cheung C L and Lieber C M 1998 Covalently functionalized nanotubes as nanometre-sized probes in chemistry and biology *Nature* **394** 52

Wu X, Liu H, Liu J, Haley K N, Treadway J A, Larson J P, Ge N, Peale F and Bruchez M P 2003 Immunofluorescent labeling of cancer marker Her2 and other cellular targets with semiconductor quantum dots *Nat. Biotechnol.* **21** 41

Xu Y and Schoonen M A A 2000 The absolute energy positions of conduction and valence bands of selected semiconducting minerals *Am. Mineral.* **85** 543

Zhang C J, Lee H W H, Kennedy I M and Risbud S H 1998 Observation of quantum confined excited states in GaN nanocrystals *Appl. Phys. Lett.* **72** 3035

Zhang J, Campbell R E, Ting A Y and Tsien R Y 2002 Creating new fluorescent probes for cell biology *Nat. Rev. Mol. Cell Biol.* **3** 906